agriculture

MDPI

Article

Factors Regulating Aggregate Stability and Soil Organic Carbon Accumulation Capacity in Abandoned Grasslands Under Combined Fertilization

Keyi Li [1,2,3], Yang Hu [4,5], Chenfeng Zheng [4], Yaoguang Han [1], Mo Chen [1], Xinping Zhu [2,6,*] and Hongtao Jia [3,7,*]

1 College of Grassland Science, Xinjiang Agricultural University, Urumqi 830052, China; likeyi5771@163.com (K.L.)
2 College of Bioscience and Resources Environment, Beijing University of Agriculture, Beijing 102206, China
3 College of Life Sciences, Xinjiang Agricultural University, Urumqi 830052, China
4 College of Resources and Environment, Xinjiang Agricultural University, Urumqi 830052, China
5 College of Natural Resources and Environment, Northwest Agricultural and Forestry University, Xianyang 712100, China
6 Key Laboratory of Urban Agriculture (North China), Ministry of Agriculture and Rural Affairs, Beijing 102206, China
7 Xinjiang Key Laboratory of Soil and Plant Ecological Processes, Urumqi 830052, China
* Correspondence: zhuxinping@bua.edu.cn (X.Z.); jht@xjau.edu.cn (H.J.); Tel.: +86-13579806286 (X.Z.); +86-13609915585 (H.J.)

Abstract

Abandoned grassland constituted a critical transitional stage during natural grassland restoration, and soil organic carbon (SOC) dynamics dominated the reconstruction of regional carbon-sink functions. However, the mechanisms underlying aggregate-associated SOC formation and stabilization under fertilization intervention in abandoned grasslands remained poorly understood. A one-year in situ fertilization control experiment was conducted using a space-for-time substitution approach in 12-year (12a) and 31-year (31a) abandoned grasslands in the Bayanbulak region. Combined inorganic–organic fertilization (NOF) used organic fertilization (OF; sheep manure) and inorganic nitrogen fertilization (NF). Aggregate stability, glomalin-related soil protein (GRSP), and soil SOC accumulation under different fertilization regimes were examined. Relative to no fertilization (CK), NOF significantly raised mechanically- and water-stable aggregate mean weight diameter (MWD) and geometric mean diameter (GMD) by 8.45–15.91% and 27.41–41.96% at 12a and 31a. Compared with CK, NOF significantly decreased the percentage of aggregate destruction (PAD) by 52.09% (12a) and 45.92% (31a). SOC mainly accumulated in LAs and SAs, and aggregate-bound SOC fell with shrinking particle size. Compared with CK, OF markedly raised bulk SOC by 12.53% (12a) and 13.97% (31a) relative to CK; OF significantly increased macroaggregate T-GRSP and EE-GRSP by 17.94–20.91% and 30.11–38.96% across 12a and 31a abandonment. Macroaggregates served as the primary storage pool for SOC and T-GRSP. Fertilization, particularly the inorganic–organic combination, substantially promoted SOC and GRSP accumulation and improved the SOC contribution of macroaggregates. GRSP was extremely positively correlated with SOC and aggregate stability. Grassland abandonment significantly strengthened the coupling between GRSP and SOC. Combined organic–inorganic fertilization improves soil structure and aggregate stability, whereas sole organic fertilization yields rapid increases in soil SOC concentration over the short term. Collectively, all fertilization treatments with organic inputs promote SOC accumulation in abandoned grasslands, which greatly benefited the restoration of degraded grasslands.

Check for updates

Academic Editor: Kui Cheng

Received: 11 September 2026
Revised: 20 October 2026
Accepted: 22 October 2026
Published: 24 October 2026

Copyright: © 2026 by the authors. Licensee MDPI, Basel, Switzerland. This article is an open access article distributed under the terms and conditions of the Creative Commons Attribution (CC BY) license.

Keywords: abandoned grassland; fertilization; soil aggregate stability; soil organic carbon; glomalin-related soil protein

1. Introduction

Large-scale ecological restoration projects have been carried out in the semi-arid and arid regions of northern and western China [1]. Abandoned artificial grasslands could undergo natural succession toward native grasslands, which served as a vital ecological approach for enhancing soil organic carbon (SOC) stocks across regional and global scales [2,3]. This process centered on the directional evolution of soil carbon cycling. As a critical regulator of SOC decomposition rate, aggregate stability provided physical protection and directly governed SOC sequestration efficiency [4]. SOC accumulation exhibited distinct stage-specific characteristics with increasing abandonment duration. Labile carbon fractions accumulated rapidly in the early restoration stage (<15-year), while the mid-to-late restoration stage (>30-year) was dominated by slow growth of stable carbon pools, during which the physical protection of SOC by soil aggregates gradually became predominant [5]. Therefore, grassland chronosequences with different abandonment durations could effectively reveal the stage transition rules of SOC sequestration mechanisms at the aggregate scale.

Soil aggregates represent the fundamental functional units for SOC storage. Aggregate stability was co-regulated by soil physicochemical properties and cementing agents, and its magnitude directly determined the resistance of SOC to decomposition. The formation of macroaggregates was the key to SOC sequestration at this scale [6,7]. Natural restoration of abandoned grasslands improved soil physicochemical properties, accumulated organic cementing agents, and promoted aggregate development as well as SOC sequestration [8]. However, natural restoration proceeded slowly with limited SOC sequestration efficiency [9,10]. Anthropogenic interventions were therefore urgently needed to accelerate restoration processes and enhance SOC accumulation.

As an efficient and readily scalable grassland management strategy, fertilization has emerged as a vital practice for regulating SOC accumulation and improving soil structure within deteriorated grasslands. Fertilization can modify key soil physicochemical properties, stimulate the synthesis of biogenic cementing substances, promote the development of soil aggregates, and further regulate the turnover and cycling of soil carbon [11]. Numerous relevant studies have confirmed that rational fertilization facilitates SOC accumulation and enhances potential SOC stabilization capacity in grassland ecosystems [11]. Nevertheless, grasslands exhibit variable short-term responses to organic fertilization, and many observations have documented its positive influences on soil aggregate stability [12]. Accumulating evidence further suggests that combined organic–mineral fertilization generally exerts stronger beneficial effects on soil aggregation compared with sole organic or inorganic fertilization regimes [13].

As a critical soil binding substance, glomalin-related soil protein (GRSP) is widely recognized for its outstanding cementing ability and structural stability, serving as a pivotal mediator connecting fertilization practices, soil physicochemical traits, aggregate structure, and SOC sequestration [14]. Originating from arbuscular mycorrhizal fungi, GRSP effectively bound microaggregates into large macroaggregate structures and alleviated aggregate slaking under wetting conditions, physically protecting soil organic carbon and thereby enhancing SOC sequestration [15,16]. As a core practice for regulating soil physicochemical properties, fertilization exerted a decisive effect on the secretion and accumulation of GRSP, and represented a critical link in modulating aggregate stability and SOC sequestration

via GRSP [17,18]. Excessive application of inorganic nitrogen and phosphorus tended to alter soil chemical environments and inhibit GRSP production. In contrast, organic fertilization improved soil physicochemical and nutrient conditions, provided precursors for cementing substances, optimized microbial habitats, facilitated GRSP accumulation and macroaggregate development, and enhanced SOC accumulation across all particle-size fractions [19]. Furthermore, prolonged grassland fallow induced variations in soil matrix physicochemical properties and aggregate structure, leading to stage-specific differences in the sensitivity of GRSP to soil environmental factors and its capacity to regulate aggregate stability [18]. Notably, grasslands at different abandonment stages possessed divergent initial soil baseline conditions, including variations in aggregate-size distribution and SOC content [20]. Differences in soil buffering capacity and baseline stocks of cementing agents were substantial, leading to marked heterogeneity in the magnitude and direction of responses of aggregate stability and SOC sequestration to fertilization regulation [21]. Despite existing advances, most previous studies separately explored the individual effects of fertilization and abandonment duration on GRSP or aggregate-associated SOC [22]. Few studies clarified the distribution patterns of GRSP across different aggregate-size fractions, nor systematically revealed the stage-dependent mechanisms regulating aggregate-associated SOC sequestration during secondary succession of grasslands.

Space-for-time substitution, also known as the chronosequence approach, is widely adopted in ecological research [23]. Its core principle employs site sequences along gradients of succession, age or environment to substitute long-term single-site monitoring and infer temporal ecological patterns and processes. This study adopted this method by collecting soil samples from grasslands with different abandonment durations to infer the temporal dynamics of soil processes during secondary succession [24]. This approach is particularly suitable for the semi-arid ecosystem investigated herein, because long-term continuous monitoring of successional trajectories of abandoned grasslands is often constrained by practical logistical limitations. Grasslands abandoned for 12 years (12a) and 31 years (31a) were selected in this study, Four fertilization treatments were established to measure soil physicochemical properties, aggregate-associated GRSP, aggregate stability and aggregate-associated SOC content. This study aimed to elucidate the mechanisms by which fertilization regulated GRSP accumulation, aggregate stability and SOC accumulation. We hypothesized that abandonment duration significantly modulated fertilization effects on aggregate stability and SOC accumulation; organic fertilization or combined organic–inorganic fertilization could improve soil physicochemical conditions, increase GRSP concentration, strengthen aggregate structure and promote SOC accumulation. This study aimed to elucidate the transmission mechanism through which fertilization affected aggregate stability and SOC accumulation by regulating soil physicochemical properties and GRSP, identify the reasonable fertilization regimes, and provide a theoretical basis and practical guidance for phased nutrient management and carbon-sink enhancement in abandoned grasslands.

2. Materials and Methods

2.1. Survey of Test Area and Sample Collection

The study area is located in the Bayanbulak alpine steppe, Hejing County, Xinjiang Uygur Autonomous Region, China. The region lies at an elevation of 2500 m, with a mean annual temperature of −4.8 °C and mean annual precipitation of 265.7 mm [25,26]. The soil was classified as silty clay loam, identified as Mat-Cryic Cambisol in the Chinese Soil Taxonomic System and Boroll in the USDA Soil Taxonomy [27,28]. We used a space-for-time substitution chronosequence approach. Grasslands with 12a and 31a of abandonment were selected as the experimental sites. We selected sampling sites with identical soil type,

topography, climatic conditions and prior land-use history to minimize confounding effects arising from site heterogeneity. The area was first reclaimed in 1974 as a 6 ha artificial grassland sown with *Avena fatua*. These sites were abandoned for ecological restoration in 1994 and 2013, corresponding to abandonment durations of 12a and 31a as of 2025. These abandoned grasslands shared the same summer grazing regime as the natural grassland sites, with an annual stocking rate of approximately 0.65 sheep ha^{-1} yr^{-1}. The current dominant species is *Elymus dahuricus*.

The experimental plots were fenced to eliminate grazing impacts for the fertilization experiment. A randomized design was implemented, with four fertilization treatments set up in each site, including no fertilization control, single-inorganic fertilizer application, single-organic fertilizer application, and combined organic and inorganic fertilizer application. Each block consisted of five replicate plots, yielding a total of 20 experimental plots. Each plot was established at a size of 2 m^2 (1 m × 2 m), with a 1 m isolation spacing between adjacent plots. The entire experimental area covered 120 m^2 (10 m × 12 m; Figure 1). Prior to fertilization, aboveground vegetation and litter on the soil surface were removed. Fertilizers were applied once in May 2024. Urea was used as the inorganic fertilizer with an application rate of 10 g/m^2 and a nitrogen content of 46.67%. To ensure uniform fertilization, the water volume of 728 $mL/m^2 \cdot a$ was calculated according to the mean annual precipitation of 265.7 mm in the study area. Urea was dissolved in 728 mL water and sprayed evenly onto the soil surface. Air-dried sheep manure was used as organic fertilizer, which contained 703.09 g/kg SOC, 21.81 g/kg total nitrogen (TN), 9.68 g/kg total phosphorus (TP), and 25.20 g/kg total potassium (TK). Based on nitrogen balance, the application rate of sheep manure was determined to be 214.12 g/m^2 (dry weight), followed by spraying an equal volume of water after uniform spreading. For the combined organic and inorganic fertilization treatment, the amounts of carbon, nitrogen and phosphorus applied equaled the sum of those in the single-inorganic and single-organic fertilizer treatments, with the same volume of water supplied. An equivalent volume of water was sprayed on the plots of the control treatment to eliminate disturbances to soil moisture (Table 1).

Table 1. Fertilizer application dosages for each treatment.

Fertilization Treatments	Actual Application Rate (g/m^2)	OC (g/kg)	N (g/kg)	P (g/kg)	K (g/kg)
No fertilization (CK)	—	0	0	0	0
Inorganic N fertilizer (NF)	10	0	4.67	0	0
Organic fertilization (OF)	214.12	87.32	4.67	2.07	5.40
Combined inorganic–organic fertilization (NOF)	5 + 107.06	43.66	4.67	1.04	2.7

Soil sampling was conducted in August 2025. Aboveground vegetation and litter were removed before collecting undisturbed soil in each plot. Composite soil samples from the 0–30 cm layer were collected using the five-point sampling method with shovels. In total, 40 homogenized soil samples were obtained (2 abandonment grasslands × 4 fertilization treatments × 5 replicates). Undisturbed soil samples were transported to the laboratory in plastic containers.

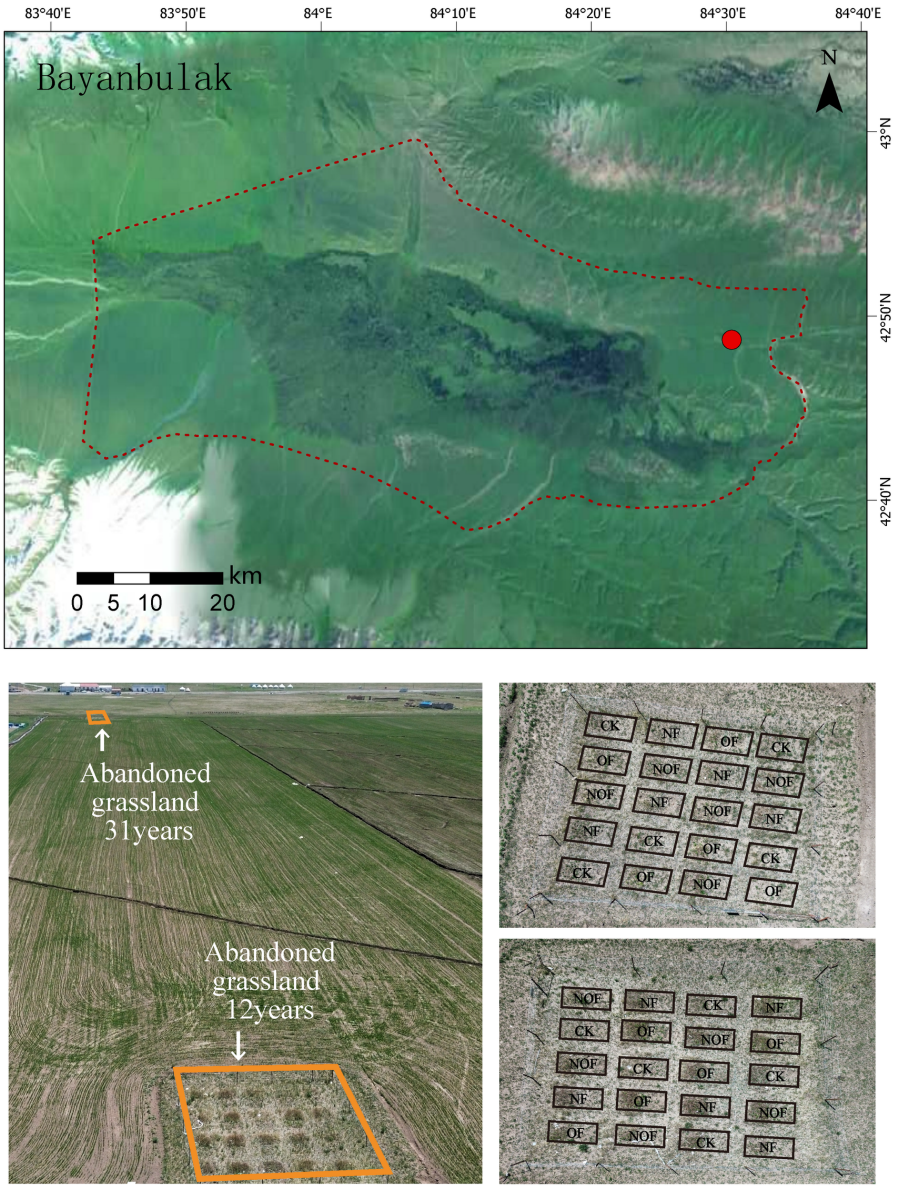

Figure 1. Map of experimental sampling sites with grasslands abandoned for 12a and 31a. The red dotted line represents the boundary of Bayanbulak, and the red solid dot indicates the location of the study area.

2.2. Measurement Method

Soil aggregates were gently broken to pass through an 8 mm sieve prior to air-drying. Soil aggregates were separated into four size fractions (>2 mm, 2–0.25 mm, 0.25–0.053 mm and <0.053 mm) via dry-sieving and wet-sieving methods, which were defined as large macroaggregates (LAs), small macroaggregates (SAs), microaggregates (Mi), and silt-clay particles (S + C), respectively. The mean weight diameter (MWD), geometric mean diameter (GMD), and percentage of aggregate destruction (PAD) of soil aggregates were calculated [29]. Higher MWD and GMD values indicate greater structural stability of soil; smaller PAD values represent more stable soil structure. The relevant calculation formulas are shown as follows:

$$\mathrm{MWD} = \sum_{i=1}^{n}(W_i X_i) \quad (1)$$

$$\mathrm{GMD} = \exp\left[\frac{\sum_{i=1}^{n}(M_i \ln X_i)}{\sum_{i=1}^{n} M_i}\right] \quad (2)$$

$$PAD = \frac{W_{d0.25} - W_{w0.25}}{W_{d0.25}} \times 100\% \quad (3)$$

where W_i is the mass percentage of aggregates in the i-th size fraction; n is the number of aggregate-size fractions; X_i is the mean diameter of aggregates in the i-th size fraction; M_i is the mass of aggregates in the i-th size fraction; and M is the total mass of soil aggregates [30].

SOC was determined by the external heating method using potassium dichromate-concentrated sulfuric acid ($K_2Cr_2O_7$-H_2SO_4). Aggregate samples were oven-dried after wet sieving prior to SOC measurement. Total soil carbon (TC) and TN were measured with an elemental analyzer (EA3000, EuroVector, Pavia, Italy). The sampling ring cutter method was utilized to establish the soil bulk density (BD). Soil pH was determined using a pH meter (Mettler Toledo FE28-Standard, Greifensee, Switzerland) at a soil-to-water ratio of 1:2.5. Available nitrogen (AN) was determined via the alkaline hydrolysis diffusion method [31]. Available phosphorus (AP) was extracted with sodium bicarbonate ($NaHCO_3$) and quantified using a spectrophotometer (Shimadzu UV-1780, Kyoto, Japan) [31]. Available potassium (AK) was extracted with ammonium acetate (CH_3COONH_4), and TK was boiled by H_2SO_4-$HClO_4$ determined by a flame photometer (Shanghai Jingke 6400A, Shanghai, China) [25].

The glomalin-related soil protein (GRSP) was determined according to Wright's method. In total, 0.5 g of soil sample was mixed with 4 mL of sodium citrate (20 mmol/·L, pH = 7.0) in a centrifuge tube, and autoclaved (TOMY SX-500,Tokyo, Japan) at 121 °C for 30 min. After centrifugation at 4 000 r/min for 5 min in a high-speed centrifuge (Eppendorf 5810R, Hamburg, Germany), the supernatant was collected for the determination of easily extractable glomalin-related soil protein (EE-GRSP) [31]. Separately, 0.5 g of soil sample was mixed with 4 mL of sodium citrate (50 mmol/L, pH = 8.0), autoclaved for 1 h, and centrifuged at 4000 r/min for 5 min to obtain the total glomalin-related soil protein (T-GRSP) extract [32,33]. This extraction procedure was repeated until the supernatant no longer exhibited the typical reddish-brown color. Finally, the absorbance of the supernatant was measured at 595 nm using the Bradford assay to determine the concentrations of EE-GRSP and T-GRSP. A calibration curve was constructed with bovine serum albumin as the standard [34].

2.3. Statistical Analysis

Experimental data were processed and visualized using Microsoft Excel 2019 (Microsoft Corporation, Redmond, USA) and Origin 2019 (OriginLab Corporation, USA). The experimental unit was the individual plot. This study included two imposed experimental factors: abandonment duration and fertilization treatment. One-way analysis of variance (ANOVA) was performed to evaluate significant differences in soil environmental factors, soil aggregate-size distribution, and aggregate-associated SOC among different treatments. Fisher's least significant difference (LSD) post hoc test ($p < 0.05$) implemented in SPSS 20.0 (IBM Corporation, USA) was used for multiple comparisons [35]. Multi-way ANOVA was used to test the main and interactive effects of fertilization treatment and aggregate-size fraction within each abandonment duration on the measured variables. Pearson correlation analysis was performed to quantify and examine the linear relationships among GRSP, aggregate stability indicators, and key soil environmental factors. The resulting correlation coefficients were further visualized in heatmaps to intuitively reveal the strength and direction of these pairwise associations across our treatments. Redundancy analysis (RDA) was performed to explore associations between soil physicochemical variables and the target variables (GRSP concentrations and aggregate stability indices). RDA was performed using the vegan package (v2.6-4) in R (v4.2.1). Separate RDA models were constructed for the 12a- and 31a-abandoned grasslands. Prior to RDA, all variables were standardized [35].

3. Results

3.1. Fundamental Physical–Chemical Soil Characteristics

In 12a- and 31a-abandoned grasslands, OF significantly increased BD by 4.45% and 5.43% relative to CK ($p < 0.05$, Figure S1a). BD slightly declined but EC rose with prolonged abandonment, while soil pH exhibited no significant inter-treatment differences at both stages ($p > 0.05$; Figure S1b,c). Compared with the CK treatment, OF significantly increased SOC by 2.41% at 12a and 6.22% at 31a, and TN by 20.08% and 43.37%, respectively (Figure S1d,f). By contrast, the soil C/N ratio decreased by 13.63% and 27.15% under OF (Figure S1g). SOC and TC fell but TN rose over time; C/N followed CK > NOF > NF > OF ($p < 0.05$). At 12a, TP and TK ranked NOF > OF > NF > CK (Figure S1h,i). AN followed OF > NOF > NF > CK across stages (Figure S1j). NF reduced AP by 39.16% (12a) and 39.72% (31a); NOF raised AK by 2.21% (12a) and 8.43% (31a, $p < 0.05$; Figure S1k,l). Overall, across 12a- and 31a-abandoned grasslands, OF reduced EC and C/N yet boosted TN and AN, NF lowered AP and AK, NOF raised TP, TK and AK, pH remained consistent among treatments, and longer abandonment significantly elevated TN but cut C/N and AK ($p < 0.05$).

3.2. Distribution Characteristics and Water Stability of Soil Aggregates

LAs dominated soil aggregates, accounting for far higher proportions than other particle sizes. Compared with CK, the NOF treatment significantly increased the proportion of mechanical LAs by 6.58% (12a) and 11.57% (31a), while markedly reducing silt-clay fractions by 2.06% and 0.76% at both abandonment ages ($p < 0.05$, Figure 2a). For water-stable LAs, NOF raised their proportion by 7.7% (12a) and 13.12% (31a) and decreased silt-clay fractions by 3.01% and 1.32% relative to CK ($p < 0.05$, Figure 2b). Overall, LA proportions were greater at 31a than 12a. Across both abandonment durations, NOF significantly enhanced mechanical and water-stable LA fractions and reduced fine S + C fractions relative to CK.

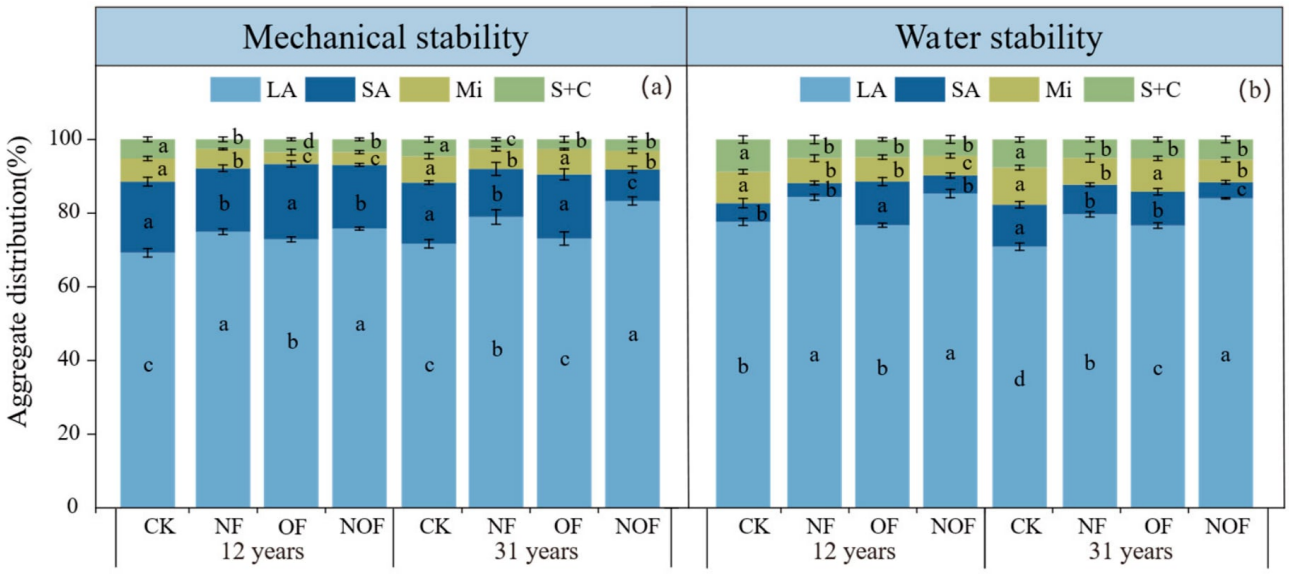

Figure 2. Responses of mass percentage of different aggregate-size fractions to varied fertilization practices on retired grassland. (**a**) Particle-size distribution of soil aggregates under mechanical stability; (**b**) particle-size distribution of soil aggregates under water stability. CK, no fertilization; NF, inorganic nitrogen fertilization; OF, organic fertilization; and NOF, combined inorganic–organic fertilization. Large macroaggregates (LAs), small macroaggregates (SAs), microaggregates (Mi), and silt-clay particles (S + C), the same below. Lowercase letters denote significant differences among fertilization treatments at ($p < 0.05$), the same below.

In grasslands abandoned for 12a and 31a, the MWD and GMD reflecting mechanical and water stability of soil aggregates followed the order of combined NOF > NF > OF > CK (Figure 3). For mechanically stable aggregate MWD, compared with CK, NOF significantly increased MWD by 8.45% at 12a ($p < 0.05$, Figure 3a), and by 13.33% at 31a ($p < 0.05$, Figure 3b). For mechanically stable aggregate GMD, NOF significantly increased GMD by 27.41% at 12a relative to CK ($p < 0.05$, Figure 3c), and by 30.34% at 31a ($p < 0.05$, Figure 3d). For water-stable aggregate MWD, NOF significantly increased MWD by 9.51% at 12a ($p < 0.05$, Figure 3e), and by 15.91% at 31a (Figure 3f). For water-stable aggregate GMD, NOF significantly increased GMD by 35.86% at 12a ($p < 0.05$, Figure 3g), and by 41.96% at 31a (Figure 3h). Meanwhile, fertilization exerted a significant effect on PAD ($p < 0.05$), with PAD ranked CK > OF > NF > NOF at both abandonment ages (Figure 3i,j). Compared with the CK treatment, NOF significantly decreased PAD by 52.09% at 12a and 45.92% at 31a ($p < 0.05$). In contrast, no significant difference in PAD was observed between the 12a- and 31a-abandoned grasslands ($p > 0.05$).

3.3. Concentrations of SOC and GRSP in Soil Aggregates

In 12a- and 31a-abandoned grasslands, aggregate-associated SOC in identical particle sizes ranked OF > NOF > NF > CK (Figure 4a,b). SOC mainly accumulated in LAs and SAs, and aggregate-associated SOC fell with shrinking particle size. OF markedly raised SOC by 12.53% (12a) and 13.97% (31a) relative to CK ($p < 0.05$). LAs dominated SOC storage, contributing 78–91% of total SOC across treatments (Table S1), and NOF further elevated their SOC contribution ratio. For CK, prolonged abandonment from 12a to 31a greatly lowered aggregate-associated SOC across all fractions and significantly reduced the LA-associated SOC contribution proportion ($p < 0.05$).

In grasslands abandoned for 12a and 31a, the contents of T-GRSP and easily extractable EE-GRSP in all aggregate-size fractions followed the order OF > NOF > NF > CK (Figure 4c–f). Abandonment duration and aggregate fraction exerted extremely significant main effects on T-GRSP and EE-GRSP concentrations ($p < 0.01$). Compared with CK, OF elevated LA T-GRSP by 17.94% (12a) and 20.91% (31a), and EE-GRSP by 30.11% and 38.96% ($p < 0.05$; Figure 4c–f). The abandonment duration–aggregate interaction was significant for T-GRSP at 12a ($p < 0.05$) and highly significant at 31a ($p < 0.01$), whereas the interaction exerted no significant influence on EE-GRSP at both succession stages ($p > 0.05$).

3.4. Relationships Between Grsp, Soil Physicochemical Properties and Soil Aggregate Stability

In 12a- and 31a-abandoned grasslands, EE-GRSP and T-GRSP across all aggregate fractions had highly significant positive linear correlations with SOC ($p < 0.01$; Figure 5). LAs exhibited the highest explanatory capacity for SOC variability, with all fractions retaining highly significant positive correlations; SOC rose linearly alongside elevated EE-GRSP and T-GRSP concentrations. For EE-GRSP, R^2 increased from 0.42–0.78 (12a) to 0.72–0.90 (31a; Figure 5a,b), while T-GRSP R^2 climbed from 0.49–0.71 to 0.77–0.85 (Figure 5c,d). Judging from the fitted R^2 values, extended abandonment reinforced GRSP-SOC linear correlations, with T-GRSP showing greater gains in fitting quality and a more stable linkage to SOC for long-term SOC accumulation.

In 12a- and 31a-abandoned grasslands, MWD and GMD correlated positively and significantly with EE-GRSP and T-GRSP in all aggregate fractions ($p < 0.05$). LA EE-GRSP and T-GRSP (LAEG, LATG) had much stronger correlations with MWD and GMD than silt-clay EE-GRSP and T-GRSP (SCEG, SCTG) at both stages ($p < 0.05$), with correlation strength rising as abandonment lengthened. All-size GRSP was positively linked to SOC, TC, TP, TK, AN and AK, yet mostly negatively correlated with AP, C/N and EC ($p < 0.05$; Figure S2).

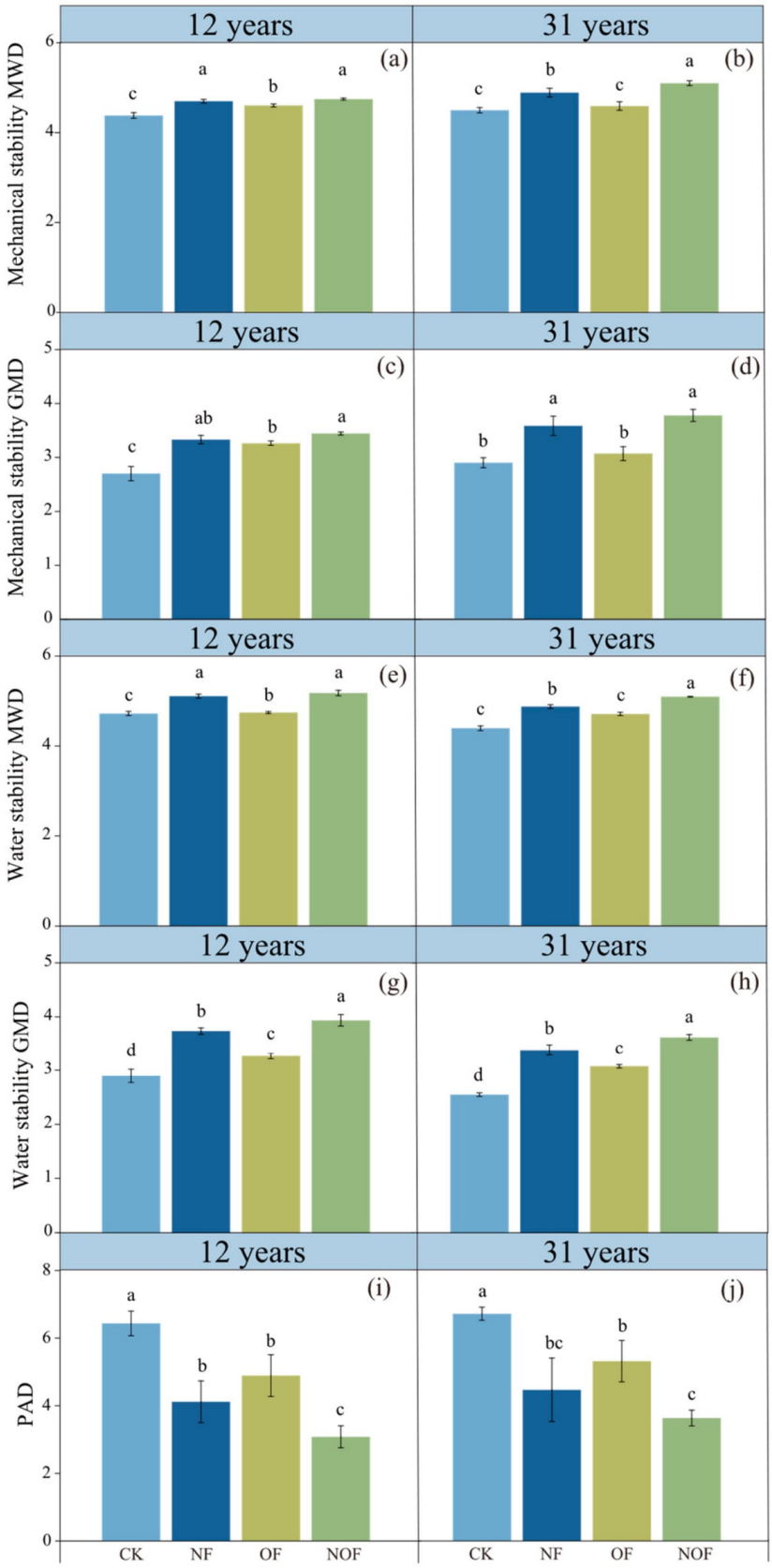

Figure 3. Effects of different fertilization regimes on mechanical stability (MWD, (**a**,**b**); GMD, (**c**,**d**) and water stability (MWD, (**e**,**f**); GMD, (**g**,**h**)) of soil aggregates, and percentage of aggregate disruption (PAD, (**i**,**j**)) in abandoned grasslands with 12-year and 31-year restoration durations. CK, no fertilization; NF, inorganic nitrogen fertilization; OF, organic fertilization; and NOF, combined inorganic–organic fertilization.

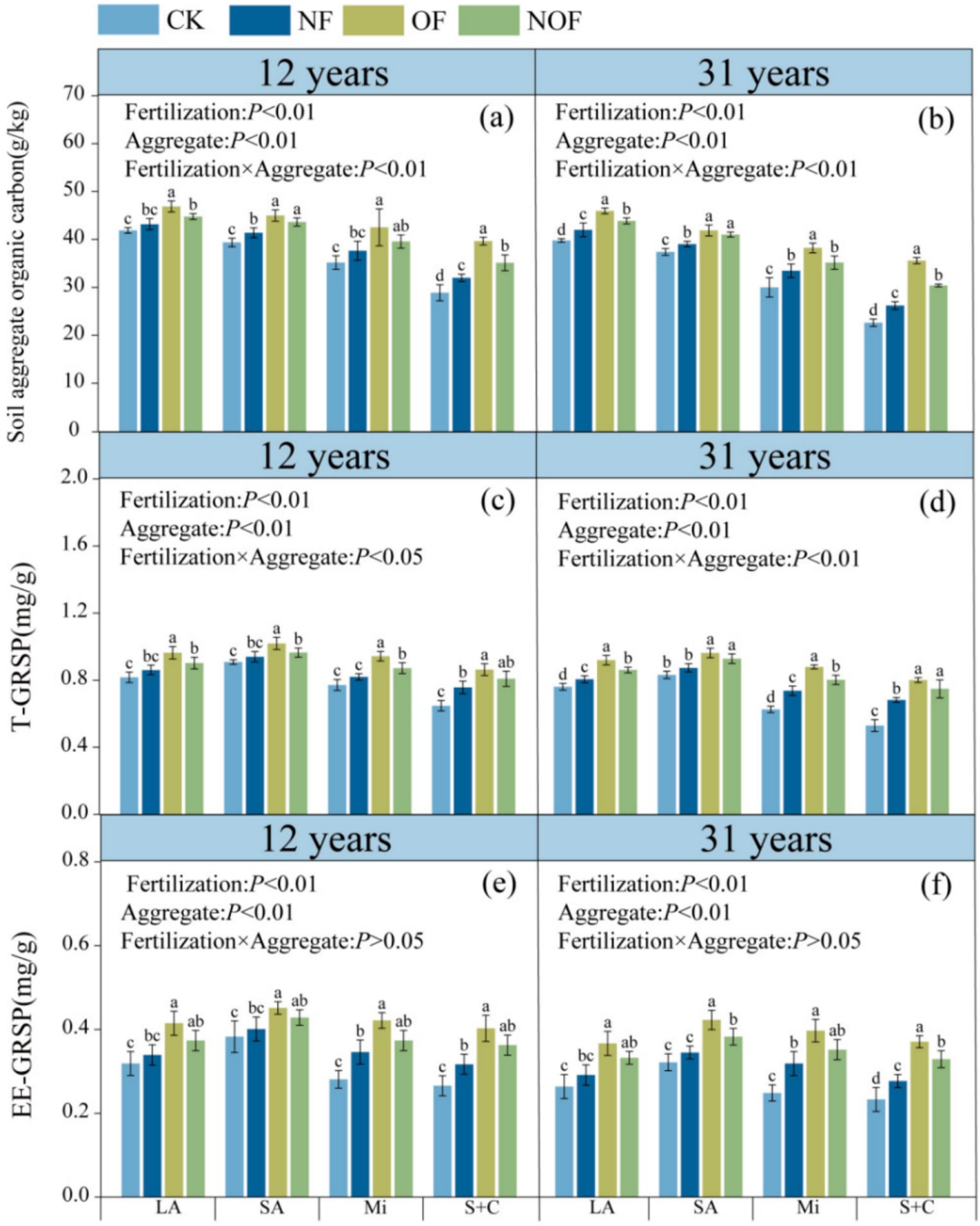

Figure 4. Soil aggregate-associated organic carbon (**a**,**b**), total glomalin-related soil protein (T-GRSP, (**c**,**d**)), and easily extractable glomalin-related soil protein (EE-GRSP, (**e**,**f**)) under different fertilization treatments after 12a and 31a abandonment. CK, no fertilization; NF, inorganic nitrogen fertilization; OF, organic fertilization; and NOF, combined inorganic–organic fertilization. Different lowercase letters indicate significant differences among fertilization treatments within the same aggregate size ($p < 0.05$). p values of two-way ANOVA for fertilization, aggregate fraction, and their interaction are shown in each panel.

RDA showed the first two axes explained 83.32% (12a) and 91.74% (31a) of total variation, adequately interpreting how soil physicochemical factors were associated with GRSP and aggregate trait shifts (Figure 6). At 12a-abandoned grassland, CK clustered on negative RDA1 with GRSP positively correlated to EC, C/N and AP. NF occupied near-zero RDA1 and high RDA2, where GRSP was positively associated with pH, MWD and GMD. OF and NOF were distributed on positive RDA1, with GRSP tightly linked

to abundant total and available nutrients. MWD and GMD were positively associated with SOC, TC and TK, while EC, AP and C/N showed negative correlations with these soil properties (Figure 6a). For 31a-abandoned grassland, RDA axes explained 91.74% variation with distinct separation across treatments. CK clustered on negative RDA1, and GRSP correlated positively with C/N, EC and AP. NF occupied negative RDA2, with GRSP negatively linked to pH, MWD and GMD. OF and NOF lay on positive RDA1 and were closely associated with TN, AK and TK, indicating that OF and NOF were co-associated with GRSP and nutrient accumulation (Figure 6b).

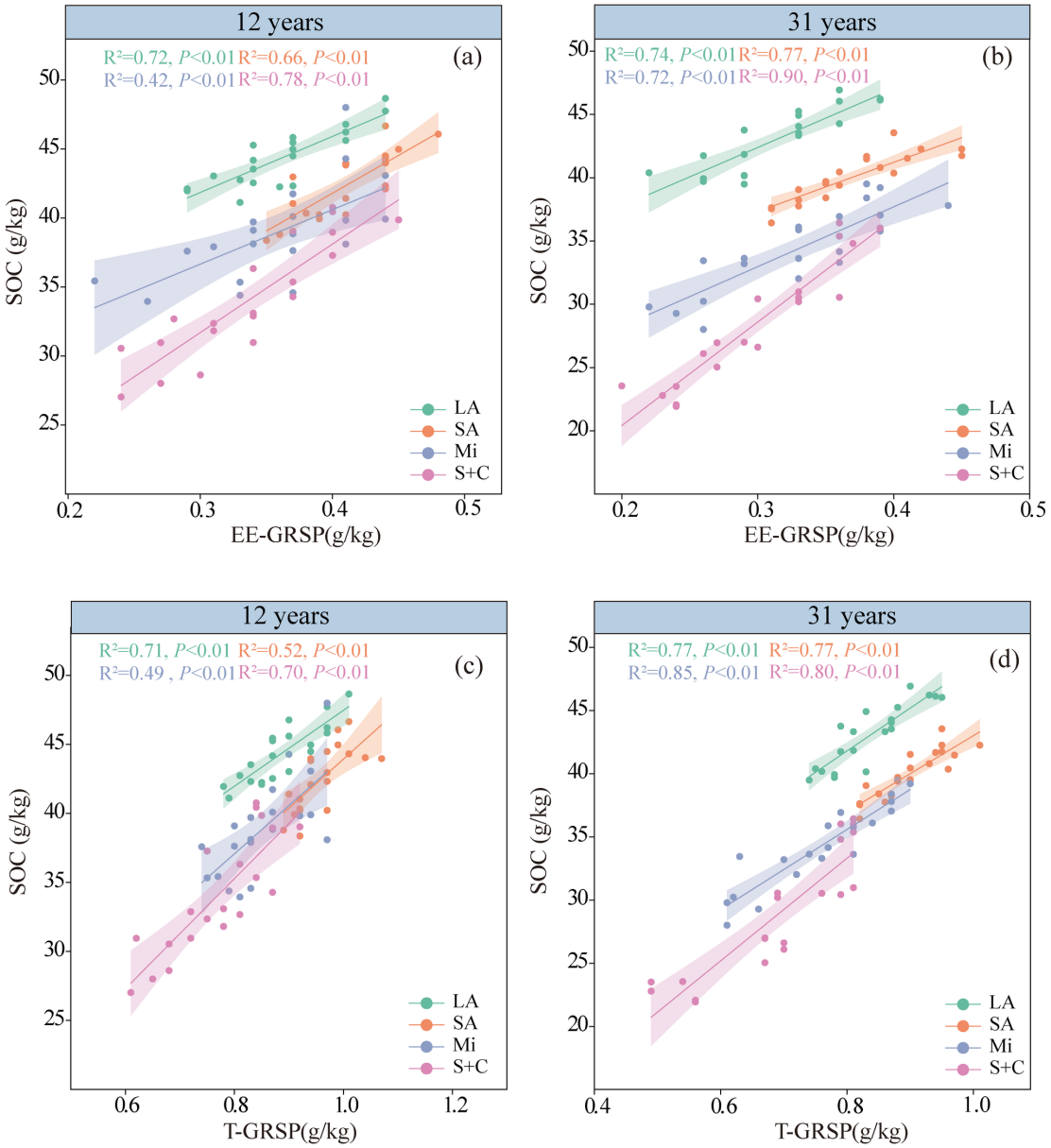

Figure 5. Linear relationships between GRSP and SOC in different aggregate fractions for 12a- and 31a-abandoned farmland. Correlations between EE-GRSP and SOC (**a**,**b**); correlations between T-GRSP and SOC (**c**,**d**). The colored solid lines represent linear regression fits for each aggregate fraction, and shaded bands indicate 95% confidence intervals. The coefficient of determination (R^2) and significance level (p) are shown for each regression.

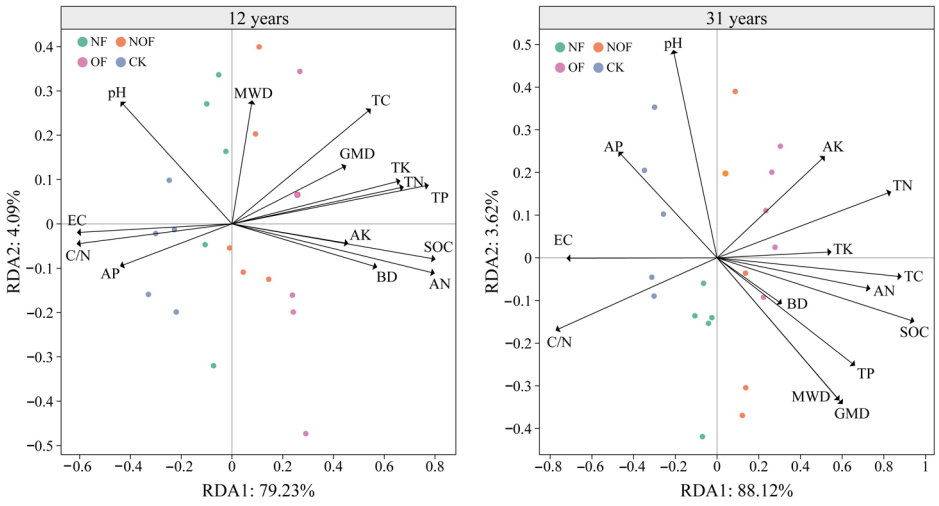

(**a**) (**b**)

Figure 6. RDA ordination diagram illustrating the differentiation characteristics of aggregate-associated GRSP, soil physicochemical properties and aggregate indicators under four fertilization treatments in abandoned grasslands with 12a (**a**) and 31a (**b**) restoration periods. Sample points represented the response patterns of GRSP under each fertilization regime, while arrow vectors denoted soil environmental factors and aggregate stability indices. MWD, mean weight diameter; GMD, geometric mean diameter; SOC, soil organic carbon; TC, total carbon; TN, total nitrogen; TP, total phosphorus; TK, total potassium; AN, available nitrogen; AP, available phosphorus; AK, available potassium; BD, bulk density; and EC, electrical conductivity. The percentages on the axes represent the proportion of total variance explained by each RDA axis.

4. Discussion

4.1. Differentiation Characteristics of Soil Physicochemical Properties as Mediated by Abandoned Grassland Succession and Fertilization

Extended abandonment duration accelerated the decomposition of soil components, facilitating a positive soil material cycle that improves soil structure and reduces bulk density (BD) [36]. However, no significant differences in soil pH were observed across all treatments, indicating that fertilization and abandonment succession did not alter soil acid–base buffering capacity, which was consistent with conclusions from most fertilization experiments on degraded grasslands [37,38]. Exogenous organic fertilizer input markedly increased SOC content in abandoned grasslands [39]. Meanwhile, fertilization might have promoted the development of soil aggregates and enhanced physical protection of SOC [19]. Our results were consistent with these observations.

In contrast, stable aggregates formed over the long term could physically protect SOC nitrogen and inhibit nitrogen mineralization, thereby potentially promoting the sustained accumulation of the recalcitrant nitrogen pool [40]. Accordingly, soil TN increased with abandonment duration, which was consistent with previous observations that nitrogen sequestration gradually proceeds during secondary succession of abandoned lands [41]. TN under sole organic fertilization was significantly higher than that under all other fertilization treatments. This phenomenon arose because organic fertilizers featured elevated C/N values and decomposed at moderate rates [42]. Nevertheless, chemical fertilization applied individually triggered intensive nitrogen mineralization, leading to substantial nitrogen dissipation through gaseous volatilization and subsurface leaching [43]. In addition, under natural abandonment conditions, sustained nutrient depletion caused the concentrations of TP and TK to be markedly lower relative to the fertilized treatments. This aligned with prior reports that nutrient pools gradually decline without external nutrient supplementation during natural vegetation restoration [44]. Combined organic–inorganic

fertilization synchronously supplied organic substrates and mineral nutrients, resulting in the highest TP and TK contents [45].

Moreover, fertilization enlarged the soil TN pool, while well-developed aggregate structures simultaneously immobilized ammonium nitrogen [46]. Combined with steady nitrogen mineralization under abandoned grasslands, the homologous supply of nitrogen substrates resulted in the synchronized dynamics of AN and TN [47]. Nevertheless, in the absence of phosphorus fertilization, soils exhibited weaker phosphorus fixation behavior, which helped retain indigenous soil AP and maintained a relatively high AP concentration level [48]. The combined inorganic–organic fertilization regime facilitated soil potassium activation, whereas sole nitrogen fertilization promoted potassium immobilization [45]. This contrast corroborates earlier findings that excessive N addition disrupts soil K transformation and shifts K toward the immobilized fraction, while organic amendments can release non-exchangeable K into available pools [49]. A sustained depletion of AK would occur in the absence of soil amelioration measures. This finding provided a reference for the rational application of fertilization practices in abandoned grasslands.

4.2. Evolution of Soil Aggregate Structure and SOC Accumulation in Abandon Grassland Mediated by GRSP, and Their Responses to Fertilization and Abandon Duration

Soil aggregate-size distribution and stability were core metrics to assess soil structure, erosion resistance and fertility [50]. Elevated macroaggregate proportion indicated better soil structure; MWD, GMD, PAD quantified aggregate stability [51]. This mechanism underpinned the macroaggregate recovery trend widely observed in land abandonment chronosequences [52,53]. Vegetation restoration, meanwhile, input persistent exogenous organic matter to sustain aggregate architecture [54]. Additionally, combined organic–inorganic fertilization supplied abundant organic binders to elevate inter-particle cohesion and promote macroaggregate development, thus improving comprehensive soil structure [55]. This fertilization maximized MWD and GMD via organic–mineral synergistic cementation to strengthen soil aggregate structural stability [56]. Single-organic fertilizer lacked mineral flocculants, while sole nitrogen fertilizer had insufficient organic binders; both hindered stable macroaggregate formation; this distinction was consistent with prior work [56,57]. Combined fertilization of inorganic and organic fertilizers significantly lowered soil PAD at both 12a- and 31a-abandoned grasslands. However, PAD values were unaffected by abandonment duration, differing from some long-term restoration observations where aggregate slaking resistance gradually improves with increasing abandonment age under unfertilized conditions [58]. This might have stemmed from a counterbalancing effect between soil aggregate water stability and mechanical stability. Specifically, the 12a-abandoned grassland exhibited lower mechanical stability but higher water stability relative to the 31a counterpart. The mechanical stability increased with restoration time, consistent with previous findings; however, such improvement generally requires more than 20–30 years to become statistically significant [21,59]. In contrast, aggregate water stability was closely associated with GRSP. While GRSP substantially improved water stability, its concentration might have declined or been redistributed over succession, potentially lowering water stability accordingly [60]. Accordingly, these opposing trends in mechanical and water stability might have jointly rendered PAD insensitive to abandonment duration.

The stable framework of macroaggregates physically protected organic carbon against microbial decomposition and mineralization loss [61]. SOC was physically protected within macroaggregates, resulting in the highest SOC concentration in macroaggregates and the lowest in silt-clay fractions [62–64]. Meanwhile, combined organic–inorganic fertilization yielded the maximum organic carbon concentrations across all aggregate fractions by elevating soil nutrients and promoting the synthesis of cementing substances to strengthen aggregate SOC accumulation capacity, which accorded with the results

reported in most previous studies [65–67]. Moreover, combined fertilization enhanced SOC accumulation in macroaggregates and helped improve potential SOC stabilization. Therefore, targeted fertilization intervention was required to maintain persistent carbon sinks in abandoned grasslands.

Carbon inputs derived from organic fertilizer can stimulate GRSP production, whereas nutrient limitation under natural abandonment suppresses mycorrhizal activity and depletes GRSP [17]. This interpretation also supports our findings. Meanwhile, macroaggregates served as the primary repository of glomalin by providing stable microbial microhabitats [68]. With increasing abandonment duration, fertilization and aggregate size exerted significant main and interactive effects on SOC and T-GRSP, respectively. However, the interactive effect of fertilization and aggregate size on EE-GRSP was non-significant. This was mainly attributed to the gradual reconstruction of soil aggregate structure during the long-term restoration of abandoned grasslands, which fundamentally drove the rising intensity of SOC interactive effects on T-GRSP along the succession chronosequence [68,69]. In contrast, EE-GRSP represented the active soluble fraction of GRSP with rapid turnover rates and certain buffering capacity against external environmental variations [18,70,71].

4.3. Linkages Between GRSP, Soil Aggregation and SOC Accumulation Under Different Fertilization Regimes Across Two Abandonment Grasslands

As a key binding agent, GRSP contributes to soil aggregate formation and SOC accumulation [72,73]. This was consistent with our finding that GRSP is strongly positively correlated with SOC. GRSP replenished SOC pools; meanwhile, it alleviated SOC mineralization loss by stabilizing soil aggregates, thereby strengthening the coupling relationship between GRSP and SOC [74]. Moreover, the positive correlations between MWD/GMD and both EE-GRSP and T-GRSP supported the widely recognized role of GRSP as a binding agent for silt-clay particles into macroaggregates. Therefore, chemically stable T-GRSP was the dominant colloid sustaining long-term SOC accumulation and soil structural stability in arid abandoned grasslands [18]. From the perspective of soil physicochemical coupling mechanisms, GRSP, a carbon-rich functional colloid, might have promoted the accretion of soil carbon pools. Fertilization elevated EE-GRSP and T-GRSP pools via regulating soil nutrients [75].

Meanwhile, GRSP could retain soil nitrogen through colloidal adsorption and mitigate nutrient leaching losses, which resulted in markedly positive correlations between GRSP and TN, as well as AN [18]. Moreover, during vegetation restoration of abandoned land, the nitrogen accumulation rate exceeded that of SOC, thereby reducing the soil C/N ratio as GRSP continued to build up. GRSP buildup was accompanied by aggregate development and modified soil pore configuration, which correlated with reduced soil BD and improved soil aeration conditions [76]. Additionally, GRSP adsorbed soluble salt ions to lower soil EC, thereby effectively alleviating the salinization risk of abandoned grasslands [77]. Early abandonment soils with relatively high carbon and nutrient availability tended to coincide with higher GRSP levels and greater aggregate stability, similar to the results reported by Zhao et al. [78]. Nevertheless, high bulk density, AP, as well as unbalanced C/N stoichiometry, greatly weakened GRSP activity and impeded the formation of soil aggregate structure [31]. Along with the advancement of secondary succession on abandoned land, the physicochemical properties of soil were progressively optimized and stabilized. Such favorable soil conditions synchronously supported the continuous accumulation of GRSP and the orderly development of soil aggregates in a coordinated manner [78–80].

RDA ordination further indicated that fertilization improved and strengthened the coupling relationships among soil nutrients, GRSP fractions, and key aggregate properties across the chronosequence of abandoned grasslands. Regardless of abandonment duration, both organic fertilization and combined inorganic–organic fertilization remained tightly

and positively associated with soil nutrient pools. This stable linkage supported the notion that fertilization can continuously stimulate GRSP production through sustained nutrient supply in abandoned grasslands, which was broadly consistent with prior reports documenting nutrient-driven promotion of GRSP formation [73]. In contrast, the NF treatment showed a significant positive correlation between GRSP and aggregate stability at 12a of abandonment, whereas this relationship turned significantly negative at 31a. This revealed that the intrinsic coupling relationship between GRSP and aggregate stability under persistent nutrient limitation gradually shifts and varies as secondary succession proceeds in these abandoned grasslands. Unlike the commonly reported static positive association, our results supported that GRSP-mediated aggregate stabilization is context-dependent, modulated by both successional age and nutrient availability [81]. Collectively, these findings demonstrated that OF and NOF represented effective fertilization strategies to sustain GRSP formation and promote aggregate development across different successional stages of abandoned grasslands.

4.4. Co-Regulation of GRSP, Soil Aggregation and SOC Accumulation by Abandonment Age and Fertilization

Short-term fertilization could rapidly regulate soil aggregate structure, GRSP accumulation, and SOC accumulation in early-stage abandoned grasslands [82]. These results were consistent with findings from long-term fertilization trials. Nevertheless, due to differences in fertilization duration, fertilizer type and soil type, we observed divergent cumulative changes in aggregate-associated SOC under our fertilization schemes across abandoned grasslands of different abandonment ages (Figure 7). Short-term abandonment (12a) increased SOC content, establishing a favorable baseline of soil nutrients, whereas combined organic–inorganic fertilization provided organic binding substrates to stimulate GRSP synthesis. Acting as a key binding agent, GRSP facilitated the transformation of microaggregates into macroaggregates, which increased MWD and GMD while reducing PAD. Macroaggregates might have physically protected SOC, thereby inhibiting microbial mineralization of SOC; concurrently, the increase in SOC might have contributed to GRSP biosynthesis. This finding was consistent with previously proposed mechanisms that might promote accelerated SOC accumulation [80,81]. Sole nitrogen fertilization reduced AP and AK, while sole organic fertilization exerted weaker effects on SOC accumulation and aggregate structural improvement relative to combined fertilization. As restoration proceeded, the unfertilized control treatment gradually lost the capacity of macroaggregates to store carbon.

Taken together, our results showed that sole organic fertilization achieved a greater increase in SOC concentration than combined organic–inorganic fertilization, whereas combined organic–inorganic fertilization was more effective at enhancing aggregate stability than sole organic fertilization. This might have been because deficient mineral nutrients under sole organic fertilization restricted organic–mineral association, thereby failing to efficiently improve soil aggregate stability [83]. Although short-term application of combined organic–inorganic fertilizer showed a weaker promotion effect on SOC than sole organic fertilizer application, it facilitated particle consolidation via nutrient complementarity, and markedly improved soil MWD, GMD and overall structural stability [84]. Short-term sole organic fertilization effectively promoted aggregate-associated organic carbon accumulation in abandoned grassland soils but exhibited limited efficacy in improving soil structural stability. In contrast, combined organic–inorganic fertilization optimized soil aggregate architecture and substantially improved aggregate stability, demonstrating divergent but functionally complementary roles of the two fertilization regimes in regulating soil structure and SOC accumulation during early restoration stages.

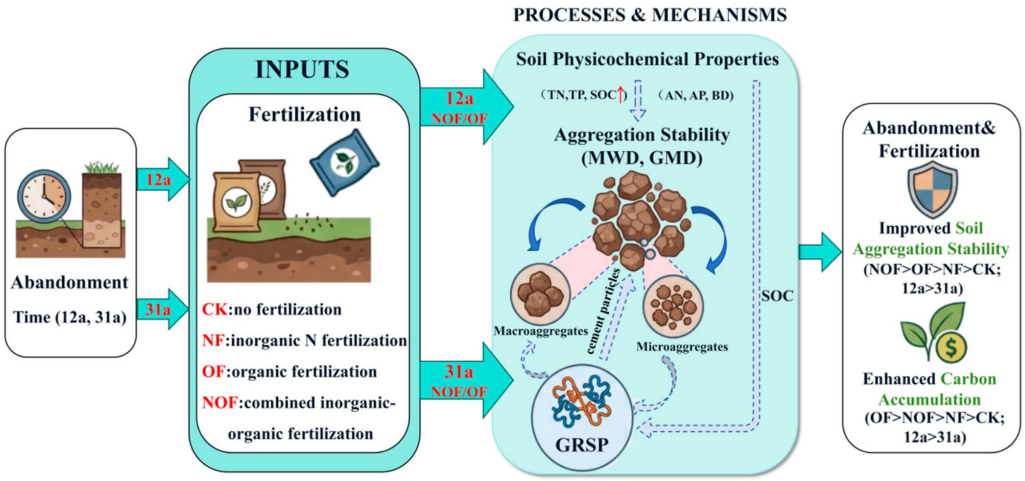

Figure 7. Conceptual framework illustrating how abandonment duration and combined fertilization regulate aggregate stability and SOC accumulation by GRSP in abandoned grasslands. Solid lines indicate relationships observed in this study. Dotted lines denote hypothesized mechanistic linkages. Green arrows denote fertilization inputs under the 12a and 31a abandonment durations, and blue arrows show the cementation and turnover relationships among macroaggregates, microaggregates, and GRSP. The positive feedback loop among GRSP, aggregate formation, and SOC accumulation represents a plausible mechanistic hypothesis derived from the present findings and the previous literature.

Although we carefully selected sampling sites with comparable topography and consistent historical land-use backgrounds, intrinsic heterogeneity in initial soil properties and plant communities inevitably persisted between the 12a- and 31a-abandoned grasslands. This constituted a well-recognized caveat of the space-for-time substitution chronosequence design, which assumed that spatial sites differed primarily in abandonment age. In addition, our short-term fertilization trial could not fully capture slow, long-term trajectories of SOC pools and aggregate turnover over succession. Accordingly, continuous multi-year in situ monitoring of combined fertilization regimes was required to validate the snapshot observations from this study and better reveal the persistent controls of nutrient addition on potential SOC stabilization and aggregate development.

5. Conclusions

This study revealed the key factors regulating overall soil aggregate stability and SOC accumulation capacity of abandoned grasslands under the combined effects of abandonment duration and fertilization. Overall, our findings partially supported the hypotheses proposed. Across both 12a- and 31a-abandoned grasslands, NOF significantly increased MWD and GMD while decreasing PAD, indicating improved water-stable aggregate structure. Fertilization was associated with elevated GRSP concentrations, alongside greater macroaggregate formation and increased SOC accumulation, with stronger responses observed in the 31a-abandoned site. GRSP was concentrated primarily within macroaggregates, acting as a key binding agent; recalcitrant T-GRSP sustained potential SOC stabilization, whereas labile EE-GRSP contributed more strongly to particle cementation. GRSP concentrations were positively correlated with SOC, nutrient availability and aggregate stability, and these synergistic relationships intensified with increasing abandonment duration. Natural succession alone depleted available nutrients, distorted soil C/N stoichiometry and failed to maintain continuous SOC accumulation. In contrast, balanced nutrient inputs from NOF alleviated nutrient limitation, optimized aggregate architecture and were potentially associated with a positive feedback loop between GRSP production, macroaggregate physical protection and SOC accumulation. Therefore, NOF and OF were

recommended as priority management practices for the short-term restoration of abandoned grasslands, especially for sites with 12a of abandonment. However, future research should involve long-term, multi-year in situ monitoring to track the effects of GRSP on soil aggregate-associated SOC accumulation under long-term combined fertilization. Overall, judicious combined organic–inorganic fertilization provides a viable pathway to accelerate soil rehabilitation and carbon-sink enhancement in degraded semi-arid grasslands beyond what natural succession alone can achieve.

Supplementary Materials: The following supporting information can be downloaded at: https://www.mdpi.com/article/10.3390/agriculture16212328/s1, Figure S1: Changes in soil physicochemical properties (a–l) under different fertilization treatments in 12-year and 31-year abandoned farmland.; Figure S2: Pearson correlation matrix among soil aggregate-stability indices; Table S1: Effects of fertilization on contribution rate of SOC in soil aggregates of abandoned grassland.

Author Contributions: K.L.: Designing experiments, sample collection and processing data, analyzing results and writing papers. Y.H. (Yang Hu): Sample collection, processing data and analyzing results. C.Z.: Sample collection and processing data. Y.H. (Yaoguang Han): Processing data. M.C.: Indoor sample determination. X.Z.: Designing experiments, supervising. H.J.: supervising. All authors have read and agreed to the published version of the manuscript.

Funding: This study was jointly supported by the National Natural Science Foundation of China (No. 31960258, No. 31560171 and No. 42507424).

Data Availability Statement: The original contributions presented in this study are included in the Supplementary Material. Further inquiries can be directed to the corresponding authors.

Acknowledgments: We were grateful to Kaihui Li, director of the Bayinbuluk Grassland Ecosystem Research Station, Chinese Academy of Sciences, and Badu, the director of the Baxilige Village Hejing County, Bayingol Mongolian Autonomous Prefecture, for their support.

Conflicts of Interest: The authors declare no conflicts of interest.

References

1. Li, C.; Fu, B.; Wang, S.; Stringer, L.C.; Wang, Y.; Li, Z.; Liu, Y.; Zhou, W. Drivers and impacts of changes in China's drylands. *Nat. Rev. Earth Environ.* **2021**, *2*, 858–873. [CrossRef]
2. Deng, J.J.; Bai, X.J.; Zhou, Y.B.; Zhu, W.X.; Yin, Y. Variations of soil microbial communities accompanied by different vegetation restoration in an open-cut iron mining area. *Sci. Total Environ.* **2020**, *704*, 135243. [CrossRef] [PubMed]
3. Karimi, N.M.T.; Gajski, D.; Jeanroy, C.G.; Verburg, P.H.; Alberti, G.; Šamonil, P. Soil Carbon Sequestration Following Natural Vegetation Recovery on Abandoned European Lands: Review and Research Needs. *Eur. J. Soil Sci.* **2026**, *77*, e70333. [CrossRef]
4. Six, J.; Elliott, E.T.; Paustian, K. Soil macroaggregate turnover and microaggregate formation: A mechanism for C sequestration under no-tillage agriculture. *Soil Biol. Biochem.* **2000**, *32*, 2099–2103. [CrossRef]
5. Liu, Y.M.; Li, W.J.; Yang, S.H.; Nummi, P.; Xu, J.Z.; Wang, D.L. Contributions of Plant- and Microbial-Derived Carbon to Soil Organic Carbon Across a Grassland Restoration Chronosequence in a Semi-Arid Typical Steppe of Inner Mongolia. *Agronomy* **2026**, *16*, 1102. [CrossRef]
6. Denef, K.; Six, J.; Merckx, R.; Paustian, K. Carbon sequestration in microaggregates of no-tillage soils with different clay mineralogy. *Soil Sci. Soc. Am. J.* **2004**, *68*, 1935–1944. [CrossRef]
7. Mustafa, A.; Xu, M.J.; Ali Shah, S.A.; Abrar, M.M.; Sun, N.; Wang, B.R.; Cai, Z.J.; Saeed, Q.; Naveed, M.; Mehmood, K.; et al. Soil aggregation and soil aggregate stability regulate organic carbon and nitrogen storage in a red soil of southern China. *J. Environ. Manag.* **2020**, *270*, 110894. [CrossRef] [PubMed]
8. Sun, L.P.; He, L.R.; Wang, G.L.; Jing, H.; Liu, G.B. Natural vegetation restoration of Liaodong oak (Quercus liaotungensis Koidz.) forests rapidly increased the content and ratio of inert carbon in soil macroaggregates. *J. Arid Land* **2019**, *11*, 928–938. [CrossRef]
9. Chang, X.F.; Chai, Q.L.; Wang, G.J.; Wu, G.L.; Zhu, Y.J.; Li, Z.W.; Yang, Y.F. Soil organic carbon accumulation in abandoned croplands on the loess plateau: Vegetation succession and SOC recovery. *Land Degrad. Dev.* **2016**, *28*, 1519–1527. [CrossRef]
10. Post, W.M.; Kwon, K.C. Soil carbon sequestration and land-use change: Processes and potential. *Glob. Change Biol.* **2000**, *6*, 317–327. [CrossRef]

11. Du, J.X.; Liu, K.L.; Huang, J.; Han, T.F.; Zhang, L.; Anthonio, C.K.; Shah, A.; Khan, M.N.; Qaswar, M.; Abbas, M.; et al. Organic carbon distribution and soil aggregate stability in response to long-term phosphorus addition in different land-use types. *Soil Tillage Res.* **2022**, *215*, 105195. [CrossRef]
12. Hurisso, T.T.; Davis, J.G.; Brummer, J.E.; Stromberger, M.E.; Mikha, M.M.; Haddix, M.L.; Paul, E.A. Rapid changes in microbial biomass and aggregate size distribution in response to changes in organic matter management in grass pasture. *Geoderma* **2013**, *193–194*, 68–75. [CrossRef]
13. Song, H.; Yang, B.; Liang, Y.; Yang, L.; Song, J.; Li, T. Combined Application of Balanced Chemical and Organic Fertilizers on Improving Crop Yield by Affecting Soil Macroaggregation and Carbon Sequestration. *Agronomy* **2024**, *14*, 2813. [CrossRef]
14. Zhang, S.X.; Li, Q.; Zhang, X.P.; Wei, K.; Chen, L.J.; Liang, W.J. Effects of conservation tillage on soil aggregation and aggregate binding agents in black soil of Northeast China. *Soil Tillage Res.* **2012**, *124*, 196–202. [CrossRef]
15. Jing, H.; Meng, M.; Wang, G.L.; Liu, G.B. Aggregate binding agents improve soil aggregate stability in Robinia pseudoacacia forests along a climatic gradient on the Loess Plateau China. *J. Arid Land* **2021**, *13*, 165–174. [CrossRef]
16. Wright, S.F.; Upadhyaya, A.; Buyer, J.S. Comparison of N-linked oligosaccharides of glomalin from arbuscular mycorrhizal fungi and soils by capillary electrophoresis. *Soil Biol. Biochem.* **1998**, *30*, 1853–1857. [CrossRef]
17. Yang, H.B.; Li, G.M.; Wu, D.; Xiao, Q.; Li, X.; Huang, Y.P.; Meersmans, J.; Colinet, G.; Xu, M.G.; Zhang, W.J. Long-term fertilization-induced increases in glomalin-related soil protein depend on phosphorus input and aggregate stability across climatic zones. *Soil Tillage Res.* **2026**, *257*, 106950. [CrossRef]
18. Zeng, J.; Wang, X.; Wang, Z.C.; Chen, F.; Fang, J.B.; Wang, H.X.; Ren, C.J.; Yang, G.H.; Zhong, Z.K.; Luo, Y.Q.; et al. Alterations in soil pH dri-ve the impact of global change on glomalin-related soil protein: A global meta-analysis. *J. Environ. Manag.* **2026**, *403*, 129221. [CrossRef] [PubMed]
19. Tian, S.Y.; Zhu, B.J.; Yin, R.; Wang, M.W.; Jiang, Y.J.; Zhang, C.Z.; Li, D.M.; Chen, X.Y.; Kardol, P.; Liu, M.Q. Organic fertilization promotes crop productivity through changes in soil aggregation. *Soil Biol. Biochem.* **2022**, *165*, 108533. [CrossRef]
20. Lv, X.H.; Tang, Q.; Han, C.; Song, M.X.; Yuan, C.; Yang, Q.Y.; Wei, J.; He, X.B.; Collins, A.L. Farmland abandonment and vegetation succession mediate soil properties but are determined by the duration of conversion. *CATENA* **2024**, *238*, 107877. [CrossRef]
21. Du, Z.; Zhou, R.; Chen, Y.; Zhan, E.R.; Chen, Y.J.; Zheng, H.; Deng, D.Z.; He, L.; Chen, D.C.; Gao, H.J.; et al. Effects of long-term vegetation restoration on soil aggregate and aggregate-associated nutrient stoichiometry of desertified grassland on the eastern Qinghai–Tibet Plateau. *Agric. Ecosyst. Environ.* **2025**, *388*, 109661. [CrossRef]
22. Lu, Y.; Wang, J.B.; Wu, G.; Wu, P.P.; Miao, Q.; Yuan, M.; Liu, C.; Sun, Z.L.; Wang, H.; Sun, Y.X. Organic Amendment Source Affects Soil Aggregation, Carbon–Nitrogen Allocation, and Wheat Yield in a Long-Term Rice–Wheat Rotation System. *Agronomy* **2026**, *16*, 1046. [CrossRef]
23. Pickett, S.T.A. *Space-for-Time Substitution as an Alternative to Long-Term Studies*; Springer: New York, NY, USA, 1989; pp. 110–135.
24. Walker, L.R.; Wardle, D.A.; Bardgett, R.D.; Clarkson, B.D. The use of chronosequences in studies of ecological succession and soil development. *J. Ecol.* **2010**, *98*, 725–736. [CrossRef]
25. Hu, Y.; Yu, G.L.; Zhou, J.Q.; Li, K.H.; Chen, M.; Abulaizi, M.; Cong, M.F.; Yang, Z.L.; Zhu, X.P.; Jia, H.T. Grazing and reclamation-induced microbiome alterations drive organic carbon stability within soil aggregates in alpine steppes. *CATENA* **2023**, *231*, 107306. [CrossRef]
26. Li, J.; Che, Y.; Chen, S.; Liu, M.; Diao, M.; Yang, C.; Jia, W. Bacillus tropicus YJ33 and Medicago sativa L. Synergistically Enhance Soil Aggregate Stability in Saline-Alkali Environments. *Microorganisms* **2025**, *13*, 1291. [CrossRef] [PubMed]
27. Li, K.Y.; Han, Y.G.; Chen, M.; Yu, G.L.; Abulaizi, M.; Hu, Y.; Wang, B.H.; Yang, Z.L.; Zhu, X.P.; Jia, H.T. Impact of Different Land-Use Types on Soil Microbial Carbon Metabolism Function in Arid Region of Alpine Grassland. *Plants* **2024**, *13*, 3531. [CrossRef] [PubMed]
28. Zheng, C.F.; Yu, G.L.; Hu, Y.; Li, K.Y.; Li, K.H.; Abulaizi, M.; Yang, Z.L.; Zhou, X.L.; Zhang, S.; Chen, M.; et al. Microbial community assembly mediated by soil organic carbon stability in aggregates under long-term enclosure alpine meadows. *Ecol. Indic.* **2026**, *189*, 115097. [CrossRef]
29. Li, S.; Zhao, J.F.; Chen, Y.; Fan, M.S.; Yu, J.; Shi, X.H. Effects of Partial Substitution of Chemical Fertilizers with Organic Fertilizers on Aggregate Stability and Organic Carbon Content in Sandy Soil. *Agriculture* **2026**, *16*, 625. [CrossRef]
30. Liu, X.; Lin, D.; Liu, Z.; Wang, H.; Qie, T.; Sun, G.; Shi, Y. Soil Particle Size Distribution Characteristics of Mechanical and Water-Stable Aggregates in Alpine Meadows Under Different Grazing Intensities. *Agriculture* **2026**, *16*, 754. [CrossRef]
31. Xie, Y.; Ma, D.H.; Zhang, Y.Q.; Cheng, Y.X.; Wang, Q.Y.; Huo, Y.W.; Tariq, S.; Zhang, J.B. Comprehensive evaluation system for amendment selection: A case study of degraded black soil improvement. *J. Environ. Manag.* **2026**, *405*, 129658. [CrossRef] [PubMed]
32. Cai, C.Y.M.; Huang, F.; Yang, Y.Y.; Yu, S.Q.; Wang, S.J.; Fan, Y.L.; Wang, Q.; Liu, W. Effects of glomalin-related soil protein driven by root on forest soil aggregate stability and carbon sequestration during urbanization in Nanchang, China. *Plants* **2023**, *12*, 1847. [CrossRef] [PubMed]

33. Zou, Y.N.; Chen, X.; Srivastava, A.K.; Wang, P.; Xiang, L.; Wu, Q.S. Changes in rhizosphere properties of trifoliate orange in response to mycorrhization and sod culture. *Appl. Soil Ecol.* **2016**, *107*, 307–312. [CrossRef]
34. Peng, S.L.; Guo, T.; Liu, G.C. The effects of arbuscular mycorrhizal hyphal networks on soil aggregations of purple soil in southwest China. *Soil Biol. Biochem.* **2013**, *57*, 411–417. [CrossRef]
35. Muñoz, N.C.; Quiroz, P.Y.; Muñoz, B.A.; Fernández, G.M. Enhancing Antimicrobial and Antioxidant Properties of Chitosan-Based Films with 1-Methylimidazolium-Chitosan. *Polymers* **2025**, *17*, 2608. [CrossRef] [PubMed]
36. Kim, S.W.; Jeong, S.W.; An, Y.J. Application of a soil quality assessment system using ecotoxicological indicators to evaluate contaminated and remediated soils. *Environ. Geochem. Health* **2020**, *42*, 1681–1690. [CrossRef] [PubMed]
37. Hao, T.X.; Zhang, Y.Y.; Zhang, J.B.; Müller, C.; Li, K.H.; Zhang, K.P.; Chu, H.Y.; Stevens, C.; Liu, X.J. Chronic nitrogen addition differentially affects gross nitrogen transformations in alpine and temperate grassland soils. *Soil Biol. Biochem.* **2020**, *149*, 107962. [CrossRef]
38. McHugh, T.A.; Morrissey, E.M.; Mueller, R.C.; Gallegos-Graves, L.V.; Kuske, C.R.; Reed, S.C. Bacterial, fungal, and plant communities exhibit no biomass or compositional response to two years of simulated nitrogen deposition in a semiarid grassland. *Environ. Microbiol.* **2017**, *19*, 1600–1611. [CrossRef] [PubMed]
39. Li, S.J.; Ye, S.; Liu, Z.Q.; Hassan, M.U.; Huang, G.Q.; Zhou, Q. How does intercropping contribute to soil organic carbon accumulation? A global synthesis. *Agric. Ecosyst. Environ.* **2024**, *374*, 109173. [CrossRef]
40. Zhang, Y.X.; Li, F.; Lu, Z.Y.; Pei, Z.F.; Zhao, H.X.; Shen, Q.G.; Hong, M. Organic amendments effects on soil aggregation and carbon sequestration in saline-alkaline croplands in China. *Agron. J.* **2023**, *115*, 2083–2095. [CrossRef]
41. Wen, L.; Li, D.J.; Yang, L.Q.; Luo, P.; Chen, H.; Xiao, K.C.; Song, T.Q.; Zhang, W.; He, X.Y.; Chen, H.S.; et al. Rapid recuperation of soil nitrogen following agricultural abandonment in a karst area, southwest China. *Biogeochemistry* **2016**, *129*, 341–354. [CrossRef]
42. Gutser, R.; Ebertseder, T.; Weber, A.; Schraml, M.; Schmidhalter, U. Short-term and residual availability of nitrogen after long-term application of organic fertilizers on arable land. *J. Plant Nutr. Soil Sci.* **2005**, *168*, 439–446. [CrossRef]
43. Wang, J.; Duan, Y.H.; Li, G.M.; Zhang, L.; Li, D.J.; Liu, K.L.; Cui, X.A.; Zhou, B.K.; Gao, H.J.; Han, X.R.; et al. Response of soil gross nitrogen mineralization to fertilization practices in China's uplands. *J. Clean. Prod.* **2024**, *480*, 144123. [CrossRef]
44. Xue, Y.; Kang, H.B.; Cui, Y.X.; Lu, S.; Yang, H.; Zhu, J.Q.; Fu, Z.J.; Yan, C.L.; Wang, D.X. Consistent Plant and Microbe Nutrient Limitation Patterns During Natural Vegetation Restoration. *Front. Plant Sci.* **2022**, *13*, 885984. [CrossRef] [PubMed]
45. Qaswar, M.; Huang, J.; Ahmed, W.; Li, D.C.; Liu, S.J.; Zhang, L.; Cai, A.D.; Liu, L.S.; Xu, Y.M.; Gao, J.S.; et al. Yield sustainability, soil organic carbon sequ-estration and nutrients balance under long-term combined application of manure and i-norganic fertilizers in acidic paddy soil. *Soil Tillage Res.* **2020**, *198*, 104569. [CrossRef]
46. Breza, L.C.; Grandy, A.S. Organic amendments tighten nitrogen cycling in agricultural soils: A meta-analysis on gross nitrogen flux. *Front. Agron.* **2025**, *7*, 1472749. [CrossRef]
47. Yang, L.; Yang, H.; Liu, L.; Yang, S.T.; Wen, D.N.; Li, X.L.; Meng, L.; Deng, Z.; Liang, J.; Lu, D.M.; et al. Vegetation Restoration Significantly Increased Soil Organic Nitrogen Mineralization and Nitrification Rates in Karst Regions of China. *Forests* **2025**, *16*, 1006. [CrossRef]
48. Zhang, G.N.; Song, J.H.; Li, T.Y.; Du, Y.N.; He, B.H. The phosphorus budget across soil, runoff, and crop in a winter wheat-summer maize rotation: Effects of long-term management practices. *Soil Tillage Res.* **2026**, *257*, 106994. [CrossRef]
49. Zhang, F.S.; Niu, J.F.; Zhang, W.F.; Chen, X.P.; Li, C.J.; Yuan, L.X.; Xie, J.C. Potassium nutrition of crops under varied regimes of nitrogen supply. *Plant Soil* **2010**, *335*, 21–34. [CrossRef]
50. Menon, M.; Mawodza, T.; Rabbani, A.; Blaud, A.; Lair, G.J.; Babaei, M.; Kercheva, M.; Rousseva, S.; Banwart, S. Pore system characteristics of soil aggregates and th-eir relevance to aggregate stability. *Geoderma* **2020**, *366*, 114259. [CrossRef]
51. Özbolat, O.; Sánchez-Navarro, V.; Zornoza, R.; Egea-Cortines, M.; Cuartero, J.; Ros, M.; Pascual, J.A.; Boix-Fayos, C.; Almagro, M.; de Vente, J.; et al. Long-term adoption of reduced tillage and green manure improves soil physicochemical properties and increases the abundance of beneficial bacteria in a Mediterranean rainfed almond orchard. *Geoderma* **2023**, *429*, 116218. [CrossRef]
52. Li, Y.; Ma, Z.M.; Liu, Y.T.; Cui, Z.L.; Mo, Q.Y.; Zhang, C.; Sheng, H.Y.; Wang, W.; Zhang, Y.K. Variation in Soil Aggregate Stability Due to Land Use Changes from Alpine Grassland in a High-Altitude Watershed. *Land* **2023**, *12*, 393. [CrossRef]
53. Mcengwa, S.; Nyambo, S.; Nyambo; Mbanjwa, V.E.; Elephant, D.E. Cropping History and Cropland Abandonment Period Influenced Levels of Soil Organic Carbon, Distribution of Aggregates and Aggregate Associated Carbon. *Land Degrad. Dev.* **2025**, *36*, 4183–4193. [CrossRef]
54. Wang, B.; Xu, G.C.; Ma, T.T.; Chen, L.; Cheng, Y.T.; Li, P.; Li, Z.B.; Zhang, Y.X. Effects of vegetation restoration on soil aggregates, organic carbon, and nitrogen in the Loess Plateau of China. *CATENA* **2023**, *231*, 107340. [CrossRef]
55. Liu, X.L.; Liu, J.G.; Huang, J.Q.; Chen, Y.F.; Zhang, L.; Qi, Y.J.; Li, W.W.; Zhu, Y. Response of Soil Aggregate Stability to Phosphorus, Nitrogen, and Organic Fertilizer Addition: A Meta-Analysis. *Sustainability* **2023**, *15*, 10601. [CrossRef]
56. Kamran, M.; Huang, L.; Nie, J.; Geng, M.J.; Lu, Y.H.; Liao, Y.L.; Zhou, F.L.; Xu, Y.H. Effect of reduced mineral fertilization (NPK) combined with green manure on aggregate stability and soil organic carbon fractions in a fluvo-aquic paddy soil. *Soil Tillage Res.* **2021**, *211*, 105005. [CrossRef]

57. Yang, C.D.; Sainju, U.M.; Li, C.; Fu, X.; Zhao, F.Z.; Wang, J. Long-Term Chemical and Organic Fertilization Differently Affect Soil Aggregates and Associated Carbon and Nitrogen in the Loess Plateau of China. *Agronomy* **2023**, *13*, 1466. [CrossRef]
58. Li, Y.Y.; Shao, M.A. Change of soil physical properties under long-term natural vegetation restoration in the Loess Plateau of China. *J. Arid Environ.* **2006**, *64*, 77–96. [CrossRef]
59. Ajayi, A.E.; Horn, R. Transformation of ex-arable land to permanent grassland promotes pore rigidity and mechanical soil resilience. *Ecol. Eng.* **2016**, *94*, 592–598. [CrossRef]
60. Cui, Z.; Xin, J.; Yang, X.; Dang, Y.; Lin, C.; Ma, Z.; Wang, K.; Wang, Z.; Zhang, Y. Contribution of Glomalin-Related Soil Protein to Soil Organic Carbon Following Grassland Degradation and Restoration: A Case from Alpine Meadow of Qinghai-Tibet Plateau. *Land* **2024**, *13*, 2223. [CrossRef]
61. Luo, X.Z.; Zhang, R.; Zhang, L.L.; Frew, A.; Yu, H.X.; Hou, E.Q.; Wen, D.Z. Mechanisms of soil organic carbon stabilization and its response to conversion of primary natural broadleaf forests to secondary forests and plantation forests. *CATENA* **2024**, *240*, 108021. [CrossRef]
62. Gelaw, A.M.; Singh, B.R.; Lal, R. Organic Carbon and Nitrogen Associated with Soil Aggregates and Particle Sizes Under Different Land Uses in Tigray, Northern Ethiopia. *Land Degrad. Dev.* **2015**, *26*, 690–700. [CrossRef]
63. King, A.E.; Congreves, K.A.; Deen, B.; Dunfield, K.E.; Voroney, R.P.; Claudia, W.R. Quantifying the relationships between soil fraction mass, fraction carbon, and total soil carbon to assess mechanisms of physical protection. *Soil Biol. Biochem.* **2019**, *135*, 95–107. [CrossRef]
64. Ojha, R.B.; Kristiansen, P.; Atreya, K.; Wilson, B. Changes in soil organic carbon f-ractions in abandoned croplands of Nepal. *Geoderma Reg.* **2023**, *33*, e00633. [CrossRef]
65. Mustafa, A.; Hu, X.; Shah, S.A.A.; Abrar, M.M.; Maitlo, A.A.; Kubar, K.A.; Saeed, Q.; Kamran, M.; Naveed, M.; Boren, W.; et al. Long-term fertilization alters chemical composition and stability of aggregate-associated organic carbon in a Chinese red soil: Evidence from aggregate fractionation, C mineralization, and 13C NMR analyses. *J. Soils Sediments* **2021**, *21*, 2483–2496. [CrossRef]
66. Wu, Y.J.; Dong, M.H.; Wang, Y.; Yu, X.M.; Wang, Z.K.; Ye, X.F. The mechanisms of microbial and soil carbon pool responses to soil aggregates improvement by different organic fertilizers. *J. Environ. Manag.* **2025**, *395*, 127814. [CrossRef] [PubMed]
67. Yang, X.; Bao, Y.W.; Li, B.W.; Wang, R.X.; Sun, C.; Ma, D.H.; Chen, L.; Zou, H.T.; Zhang, J.B. Effects of fertilization applications on soil aggregate organic carbon content and assessment of their influencing factors: A meta-analysis. *CATENA* **2024**, *242*, 108135. [CrossRef]
68. Liu, H.F.; Wang, X.K.; Liang, C.T.; Ai, Z.M.; Wu, Y.; Xu, H.W.; Xue, S.; Liu, G.B. Glomalin-related soil protein affects soil aggregation and recovery of soil nutrient following natural revegetation on the Loess Plateau. *Geoderma* **2020**, *357*, 113921. [CrossRef]
69. Zang, Z.F.; Zhang, Y.; Deng, S.J.; Yang, K.; Tang, F.H.; Lv, Y.; Zhao, W. Depth-dependent effects of aggregate-associated organic, inorganic carbon, and stoichiometry on soil structural stability following farmland abandonment. *CATENA* **2025**, *252*, 108864. [CrossRef]
70. Ling, Q.M.; Wu, H.Q.; Xie, L.; Zhao, Y.; Huang, Q.B.; Zhang, Q.; Liu, J.; Hu, P.L.; Tang, T.G.; Xiao, J.; et al. Advances, Challenges, and Perspectives in Glomalin-Related Soil Protein Research. *Microorganisms* **2025**, *13*, 740. [CrossRef] [PubMed]
71. Sun, X.Y.; Xing, Y.J.; Yan, G.Y.; Liu, G.C.; Wang, X.C.; Wang, Q.G. Dynamics of glomalin-related soil protein and soil aggregates during secondary succession in the temperate forest. *CATENA* **2024**, *234*, 107602. [CrossRef]
72. Cissé, G.; Oort, F.; Chenu, C.; Essi, M.; Staunton, S. Is the operationally defined fraction of soil organic matter, "GRSP" (glomalin-related soil protein), stable in soils? Evidence from trends in long-term bare fallow soil. *J. Soil Sci. Plant Nutr.* **2020**, *72*, 1101–1112. [CrossRef]
73. Luo, X.Z.; Zhang, L.L.; Lambers, H.; Hossain, M.A.; Liu, S.T.; Yu, H.X.; Kuang, Y.W.; Wen, D.Z.; Hou, E.Q. Global change reshapes glomalin-mediated soil carbon sequestration by influencing plant inputs. *Funct. Ecol.* **2026**, *40*, 655–667. [CrossRef]
74. Yang, H.B.; Wang, G.S.; Wang, J.; Xiao, Q.; Li, Z.Y.; De-Clerck, C.; Meersmans, J.; Colinet, G.; Zhang, W.J. No-tillage facilitates soil organic carbon sequestration by enhancing arbuscular mycorrhizal fungi-related soil proteins accumulation and aggregation. *CATENA* **2024**, *245*, 108323. [CrossRef]
75. Zhong, Z.L.; Wang, W.J.; Wang, Q.; Wu, Y.; Wang, H.M.; Pei, Z.X. Glomalin amount and compositional variation, and their associations with soil properties in farmland, northeastern China. *J. Plant Nutr. Soil Sci.* **2017**, *180*, 563–575. [CrossRef]
76. Gao, W.Q.; Wang, P.; Wu, Q.S. Functions and Application of glomalin-related soil proteins: A review. *Sains Malays.* **2019**, *48*, 111–119. [CrossRef]
77. Zhang, Z.H.; Wang, Q.; Wang, H.; Nie, S.M.; Liang, Z.W. Effects of soil salinity on the content, composition, and ion binding capacity of glomalin-related soil protein (GRSP). *Sci. Total Environ.* **2017**, *581-582*, 657–665. [CrossRef] [PubMed]
78. Zhao, X.; Wang, C.L.; Zhao, J.; Hou, B.B.; Li, Y.R.; Qiu, X.Q.; Song, P.P.; Wang, J.Q. Glomalin-Related Soil Protein and Its Relationship with Organic Carbon and Nitrogen in Water-stable Aggregates in Abandoned Agricultural Lands. *J. Energy Nat. Resour.* **2019**, *8*, 37–44. [CrossRef]

79. Emran, M.; Naeim, H.; Rashad, M.; Gispert, M. Seasonal changes in soil carbon storage capacity and glomalin-related soil protein under different agricultural activities, abandonment, and wildfire occurrence in Mediterranean region. *J. Saudi Soc. Agric. Sci.* **2022**, *21*, 359–371. [CrossRef]
80. Singh, A.K.; Rai, A.; Singh, N. Effect of long term land use systems on fractions of glomalin and soil organic carbon in the Indo-Gangetic plain. *Geoderma* **2016**, *277*, 41–50. [CrossRef]
81. Yang, Y.; Zhang, J.J.; He, J.; Shen, Y.; Yang, X. Glomalin-related soil proteins respond negatively to fertilization and fungicide application in China's arid grassland. *Eur. J. Soil Biol.* **2023**, *119*, 1164–5563. [CrossRef]
82. Zong, D.L.; Quan, Y.; Penttinen, P.; Qi, L.; Wang, J.T.; Tang, X.Y.; Xu, K.; Chen, Y.X. Organic Amendments Drive Soil Organic Carbon Sequestration and Crop Growth via Microorganisms and Aggregates. *Agronomy* **2025**, *15*, 2919. [CrossRef]
83. Abdalla, K.; Gaiser, T.; Seidel, S.J.; Pausch, J. Soil organic carbon and nitrogen in aggregates in response to over seven decades of farmyard manure application. *J. Plant Nutr. Soil Sci.* **2023**, *186*, 253–258. [CrossRef]
84. Zhang, C.; Zhao, X.; Liang, A.J.; Li, Y.Y.; Song, Q.Y.; Li, X.Y.; Li, D.P.; Hou, N. Insight into the soil aggregate-mediated restoration mechanism of degraded black soil via biochar addition: Emphasizing the driving role of core microbial communities and nutrient cycling. *Environ. Res.* **2023**, *228*, 115895. [CrossRef] [PubMed]

Disclaimer/Publisher's Note: The statements, opinions and data contained in all publications are solely those of the individual author(s) and contributor(s) and not of MDPI and/or the editor(s). MDPI and/or the editor(s) disclaim responsibility for any injury to people or property resulting from any ideas, methods, instructions or products referred to in the content.